Catalysis on Ruthenium Clusters Supported on CeO_2 or Ni-Doped CeO_2: Adsorption Behavior of H_2 and Ammonia Synthesis

Yasuo Izumi,* Yasuhiro Iwata, and Ken-ichi Aika*

Department of Environmental Chemistry and Engineering, Interdisciplinary Graduate School of Science and Engineering, Tokyo Institute of Technology, 4259 Nagatsuta, Midori-ku, Yokohama 226, Japan

Received: September 6, 1995; In Final Form: March 14, 1996[⊗]

Catalysis on Ru clusters supported on CeO_2 or Ni-doped CeO_2 was investigated. $Ru_3(CO)_{12}$ was reacted with CeO_2, followed by heating in vacuum at 673 (**i**) or 813 K (**ii**) and then in H_2 at 588−1073 K (T_{H_2}). Activities of both catalysts had the T_{H_2} dependence, which has a maximum at $T_{H_2} = 873$ K for ammonia synthesis. The rates on **i** were faster than those on **ii** by a factor of 2.0−1.1 in the range of $T_{H_2} = 588$−973 K. On a sample in which $Ru_3(CO)_{12}$ was supported on previously reduced Ni/CeO_2 (in H_2 at 773 K) **iii**, the highest synthesis rate was 1.5×10^{-3} mol h^{-1} g_{cat}^{-1} at $T_{H_2} = 588$ K on **iii**. The activity order **iii** > **i** > **ii** can be understood in terms of two factors: (A) reduction extent of support and (B) number of active Ru sites. The two factors conflicted with each other when the treatment temperature in H_2 increased. By heating the samples in H_2 up to 873 K to satisfy factor A, the aggregation of Ru clusters for **i** or physical blocking of surface Ru sites by CeO_{2-x} for **ii** occurred: factor B was not satisfied. The two factors should be optimized in catalyst **iii**, where the support cerium oxide was thoroughly reduced through the doped Ni. On reduced Ni/CeO_2, the Ru cluster implantation can be done at low temperature (588 K). Obtained values of r_{Ru-Ru} at 2.62 Å ($N = 7.1$) and $r_{Ru-O(s)}$ (O(s) is the oxygen atom at surface) at 2.12 Å ($N = 1.2$) by EXAFS for Ru_3−Ni/CeO_2 suggested a flat Ru cluster model comprised of several Ru atoms on reduced Ni/CeO_{2-x} surface. The H(a)/Ru_{total} ratio exceeded unity for catalysts **i** and **iii**, suggesting new H adsorption sites. The temperature-programmed desorption for hydrogen (simultaneous desorption of HD and D_2 for **iii** at 330−430 K suggested that the H at the new site and H on Ru surface were exchangeable above 330 K. The "reservoir" effect of the new site for H on catalysis is discussed in relation to new kinetic design of hydrogenation catalyst.

Introduction

Recently, we studied hydrogen adsorption and ammonia synthesis on Ru cluster catalysts by means of EXAFS (extended X-ray absorption fine structure) and FTIR (Fourier transform infrared spectroscopy).[1−3] Several adsorption sites of H were detected by FTIR.[1] The *in situ* structure change of Ru clusters was observed by the interaction with H_2 by EXAFS.[2] The promotion of ammonia synthesis was suggested by elongating the Ru−Ru bonding distance to facilitate the dissociative adsorption of N_2.[2,3]

The H adsorption was examined for Rh/TiO_2[4] and Ru/SiO_2[5] by solid-state ^{1}H-NMR. Two peaks were observed for Rh/TiO_2 when heated in H_2 above 573 K. The α peak around $\delta = -130$ ppm was assigned as H atom on Rh particles on the basis of P_{H_2} dependence and spin−lattice relaxation time T_1. The peak intensity decreased when the sample was heated in H_2 above 723 K in relation to the SMSI (strong metal−support interaction) effect. A part of β peak around 0 ppm was implied as "weakly bound H" on Rh particles present at relatively higher P_{H_2} (>2 kPa) compared to α peak H. Two peaks were observed for Ru/SiO_2 around −60 (α) and −30 ppm (β) in H_2.[5] The α and β peaks were assigned as H on Ru particles and "weakly bound H" on Ru particles, respectively, on the basis of heat of adsorption, T_1, and H/Ru(s) ratio. The β peak was only observed at $P_{H_2} > 13$ kPa. The weakly bound H was implied to have an interaction with lower coordination Ru sites because the β peak population increased as the Ru particle size decreased.

CeO_2 is an effective promoter or support of Ru catalysts, and the importance of metal−support interaction is often implied when reduced at high temperatures. In this paper, we report promoted catalysis over Ru clusters supported on CeO_2 or on Ni-doped CeO_2 as a first objective. The support was reduced at high temperatures (∼873 K) in H_2 (CeO_2) or at moderate temperatures (623−773 K) by spiltover H atoms from doped Ni (Ni/CeO_2). The major control factors of ammonia synthesis should be the number of active sites, the nature of the Ru/support interface, and the electronic effect of support.[3] The catalyst preparation procedure, reacting the $Ru_3(CO)_{12}$ with previously reduced Ni-doped CeO_2, optimized these control factors.

The second objective is the clarification of the promoted reaction mechanism. The hydrogen uptake exceeded unity for Ru clusters on CeO_2 or Ni-doped CeO_2. We propose the condensation of H atoms at the interface between Ru clusters and the reduced CeO_{2-x} surface. The "reservoir" effect of the interface site on catalysis is discussed.

Experimental Section

Cerium oxide was prepared from a 0.2 mol L^{-1} $Ce(NO_3)_3 \cdot 6H_2O$ (Wako, 99.9%) solution. The 5% ammonia was added until the pH of solution was 10. The obtained $Ce(OH)_4$ was filtered and repeatedly washed. Yellow powder of CeO_2 (BET surface area 57 m^2 g^{-1}) was obtained by heating $Ce(OH)_4$ in air (4 h), evacuating (1 h) at 773 K, and then treating in O_2 at 290 K. $Ru_3(CO)_{12}$ (**1**) was interacted with CeO_2 in distilled THF (tetrahydrofuran) (Wako, Special Grade) at 290 K for 2 h, with the subsequent removal of THF in vacuum (Ru_3/CeO_2). The obtained CeO_2 was impregnated with $Ni(NO_3)_2 \cdot 6H_2O$ (Wako, 99.9%) to give 0.25 wt % Ni and treated in H_2 (12 h) at 773 K, followed by a procedure similar to the case of Ru_3/CeO_2 (Ru_3−Ni/CeO_2). The loading of Ru was 1.7 wt %. All procedures of sample preparation and transfer were performed

* To whom correspondence should be addressed. E-mail: yizumi@chemenv.titech.ac.jp.

[⊗] Abstract published in *Advance ACS Abstracts,* May 15, 1996.

S0022-3654(95)02602-5 CCC: $12.00

in argon (99.99%) or in vacuum. Incipient supported clusters were heated (elevating rate of temperature 4 K min^{-1}) in vacuum up to 673 or 813 K, followed by the treatment in H_2 for 1 h (588−1073 K). The catalysts were denoted as Ru_3−Ni/CeO_2-673ev, for example, where the evacuation temperature was noted. Subsequent treatment temperature in H_2 (T_{H_2}) is noted in each description.

The conventional Ru/CeO_2 catalyst was prepared from **1** *in air*. **1** was interacted with CeO_2 and decomposed (the color of the solution turned from orange to dark yellow) in THF for 12 h (1.0 wt % Ru). After evaporation of the THF, the powder was heated in O_2 (1 h) and then in H_2 (1 h) at 773 K before being used as catalyst. The weight of the catalyst was 0.015−0.030 g for Ru_3/CeO_2, Ru_3−Ni/CeO_2, and conventional Ru/CeO_2.

The ammonia synthesis reactions were carried out under 101 kPa of reaction gas ($P_{H_2}/P_{N_2} = 3.0$) at 588 K in a flow system (flow rate 60 cm^3 min^{-1}). The produced ammonia was analyzed by the decrease of electron conductivity (1.7−0.8 mS·cm^{-1}) in the H_2SO_4 solution (<0.004 N). The linearity of the correlation between the produced amount of NH_3 and the decrease of electron conductivity was checked. The chosen reaction temperature was relatively low (588 K) to realize differential working conditions. The catalytic rates were stable in 36 h, and the rates at 2 h were listed for all the catalysts in this paper. The rates on Ru_3/CeO_2-673ev and Ru_3−Ni/CeO_2-673ev catalysts were relatively unstable only when treated in H_2 at lower temperatures (588−673 K) before catalysis. They increased in 2 h (within 30%), and a smaller increase was observed during 2−10 h (within 10%).

Hydrogen uptake (ν) measurements were carried out in a closed circulating system connected to the manometer. The equilibrium gas pressure (P) was varied in the range 1.3−20 kPa, and the b of adsorption isotherm

$$\nu^{-1} = (ab)^{-1}P^{-1/2} + b^{-1}$$

was obtained by the extrapolation of obtained data (five to seven points; a is a constant). The samples were kept in ice (273 K) during measurements. As fast uptake (adsorption on Ru + hydrogen spillover from Ru to support surface) terminated in 1 h followed by linear increase of uptake during 1−10 h (hydrogen spillover), uptake on Ru (ν) was estimated by subtracting the H spillover amount during initial 1 h from total (observed) uptake amount at 1 h. The temperature-programmed desorption (TPD) was monitored in the closed circulating system connected to the mass. The samples were treated (i) in 76 kPa of H_2 (1 h) at 293 K, evacuated (0.5 h) at 293 K, and then treated in 76 kPa of D_2 (1 h) at 293 K (adsorption A), or (ii) treated in D_2 at 293 K (1 h) (adsorption B). The elevation rate of temperature was 4 K min^{-1}.

The EXAFS spectra of Ru K edge were measured at the beamline 10B and 6B (2.5 GeV, current 360−260 mA) of the Photon Factory in the National Laboratory for High Energy Physics (Proposal No. 93G150). The X-ray radiation was monochronized through double crystals of Si(311), and the spectra were obtained in transmission mode with ionization chambers at 100−293 K. The sample was transferred to an EXAFS Pyrex cell ($0.073 < \Delta\mu t < 0.25$) with Kapton films. The analysis was performed by the program EXAFSH written by Yokoyama, Hamamatsu, and Ohta (the University of Tokyo, 1994).[2] The background subtraction was performed by calculating the cubic spline with three blocks, and the obtained function $\mu t(k) - \mu_0 t(k)$ was normalized by using Victoreen parameter $\mu_0(\lambda) = C\lambda^3 - D\lambda^4$. The Fourier transform (FT) of the k^3-weighted EXAFS oscillation was carried out over the range of

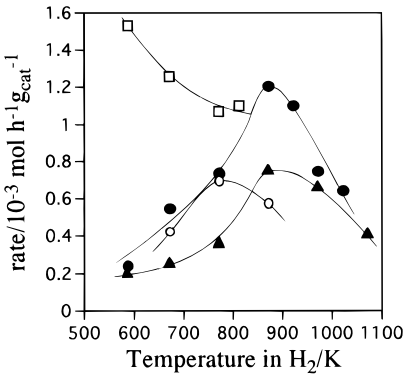

Figure 1. Dependence of ammonia synthesis rates at 588 K on hydrogen treatment temperature (T_{H_2}) over Ru_3/CeO_2-673ev (●), Ru_3/CeO_2-813ev (▲), Ru_3−Ni/CeO_2-673ev (□), and conventional Ru/CeO_2 (○).

$k_{min} = 3$ and $k_{max} = 12.6-13.5$ $Å^{-1}$. The Hanning function was multiplied by k-width of $(k_{max} - k_{min})/20$ on both ends. The inverse FT was performed in the r-range of $r_{min} = 1.04-1.36$ and $r_{max} = 2.71-2.98$ Å multiplied by the Hanning function with the r-width of 0.1 Å on both ends. The curve-fitting analysis was performed in the k-region of 4−12 $Å^{-1}$ on the basis of plane wave single scattering theory, using empirical phase shift and amplitude functions extracted from **1** for Ru−C bond, Ru powder for Ru−Ru bond, RuO_2 for Ru−O and Ru··· Ru (next-nearest coordination in RuO_2) bonds, and [$RuCl_2$-$(CO)_3$]$_2$ for Ru(−C−)O bond. The EXAFS spectra for these reference compounds were taken at room temperature. The residual factor (R_f) was calculated by the following equation

$$R_f = \int |k^3\chi^{obs}(k) - k^3\chi^{calc}(k)|^2 dk / \int |k^3\chi^{obs}(k)|^2 dk$$

The impurities (as molecular content) for the H_2 (99.99%, Toyo Sanso Co., Ltd.) and D_2 (99.99%, Syoko Co., Ltd.) gas were H_2O < 10, N_2 < 50, O_2 < 10, CO < 10, CO_2 < 10 ppm, and total hydrocarbons < 10 ppm (as carbon content). The deuterium content in total hydrogen was >99.8% for the D_2 gas. The gas was introduced to the EXAFS or IR cell after purification by passage through a liquid nitrogen trap.

The supported Ru clusters were suspended in ethanol (exposed in air during few minutes), and mounted on a TEM (transmission electron microscope) apparatus (JSM-T220, JEOL). The dispersion (D) of a Ru particle was estimated from the average diameter of Ru particles ($2d$) by TEM by using the following equation assuming the closest packed structure of Ru surface (Avogadro number N_A, molecular weight MW, interatomic distance r_{Ru-Ru}, and the density ρ of Ru).

$$D = \frac{4\pi d^2/(\sqrt{3}/2)r_{Ru-Ru}^2}{(4/3)\pi d^3 \rho N_A/MW} = \frac{6.7}{d/Å} \quad (1)$$

Results

Catalysis. When incipient Ru_3/CeO_2 cluster was heated in vacuum, the carbonyl ligands were totally desorbed as CO (and a few CO_2) until 673 K. Figure 1 shows ammonia synthesis rates at 588 K on Ru_3/CeO_2 heated in vacuum at 673 or 813 K. At $T_{H_2} = 588$ K, the rate for Ru_3/CeO_2-673ev was faster by 1.2 times than that for Ru_3/CeO_2-813ev (Table 1a,c).

The two cluster catalysts were treated in hydrogen (76 kPa) between 673 and 1073 K (Figure 1 and Table 1). The rates on Ru_3/CeO_2-673ev had a maximum at $T_{H_2} = 873$ K. Similarly, the rate over Ru_3/CeO_2-813ev reached a maximum at $T_{H_2} = 873$ K. The maximum synthesis rate for Ru_3/CeO_2-813ev was 63% of the maximum for Ru_3/CeO_2-673ev (Figure 1), suggest-

TABLE 1: Rates of Ammonia Synthesis on Ru Catalysts Supported on CeO_2[a]

entry	catalysts	T_{H_2}/K	rate/10^{-3} mol h^{-1} g_{cat}^{-1}
a	Ru_3/CeO_2-673ev	588	0.24
b		873	1.2
c	Ru_3/CeO_2-813ev	588	0.20
d		873	0.75
e	Ru_3-Ni/CeO_2-673ev	588	1.5
f	conventional Ru/CeO_2	773	0.69

[a] Temperature = 588 K. Total pressure = 101 kPa, $P_{N_2}/P_{H_2} = 1/3$.

TABLE 2: Amounts of Hydrogen Uptake for Ru Catalysts Supported on CeO_2

catalysts	T_{H_2}/K	H/Ru_{total}[a] (molar ratio)
Ru_3/CeO_2-673ev		1.5
	588	1.2
Ru_3-Ni/CeO_2-673ev		4.3
	588	4.1
conventional Ru/CeO_2	773	0.5

[a] By manometer, at 1 h in H_2 (1.3−20 kPa) at 273 K. The amount of H spillover for 1 h was subtracted from the observed total uptake at 1 h.

ing that the heating in severe condition (813 K in vacuum) induced the aggregation of Ru clusters and reduced the number of surface active sites. The rates on conventional Ru/CeO_2 are also shown in Figure 1. It produced ammonia at rates similar to those of Ru_3/CeO_2-673ev around $T_{H_2} = 673-773$ K, but the rate began to decrease above $T_{H_2} = 773$ K.

The synthesis rates on Ru_3-Ni/CeO_2-673ev were faster than the others in all the range of T_{H_2} (Figure 1). In contrast to the T_{H_2} dependence for other catalysts, the rate on Ru_3-Ni/CeO_2 monotonously decreased with the increase of T_{H_2}. The maximum rate at $T_{H_2} = 588$ K (Table 1e) was larger than 9.9×10^{-4} mol h^{-1} g_{cat}^{-1} on $[Ru_6N]-Cs^+/MgO$ (2.5 wt % Ru, 101 kPa)[3] or 6.9×10^{-4} mol h^{-1} g_{cat}^{-1} on $Ru-Cs^+/MgO$ (2 wt % Ru, 80 kPa)[6] at 588 K, suggesting super-catalytic activity of Ru_3-Ni/CeO_2 which can exceed the present industrial catalysts under the reaction conditions in this work.

The isotope effects of hydrogen were examined for ammonia synthesis in $N_2 + H_2$ and in $N_2 + D_2$. In the case of Ru_3/CeO_2-673ev and Ru_3-Ni/CeO_2-673ev heated in H_2 at 588 K, strong inverse isotope effects ($r_{D_2}/r_{H_2} = 2.0-2.2$) were observed. On the other hand, Ru_3/CeO_2-673ev exhibited no isotope effect when heated in H_2 at 773 K. Also, conventional Ru/CeO_2 had no isotope effect, similar to other conventional Ru catalysts.[3]

Hydrogen Uptake and TPD Measurements. Hydrogen uptake was measured on Ru_3/CeO_2-673ev and Ru_3-Ni/CeO_2-673ev before and after hydrogen treatment (Table 2). Compared to 0.5 for conventional Ru/CeO_2, the H/Ru_{total} ratio exceeded unity for Ru_3/CeO_2-673ev (=1.5). After in H_2 at 588 K, the value decreased to 1.2. The H/Ru_{total} value reached 4.3 for Ru_3-Ni/CeO_2-673ev and slightly decreased to 4.1 by the hydrogen treatment at 588 K. No hydrogen was adsorbed on metal-*unsupported* cerium oxide heated in vacuum at 673−813 K and/or in H_2 at 588−773 K.

The TPD of hydrogen was measured for Ru_3/CeO_2-673ev, Ru_3-Ni/CeO_2-673ev, and conventional Ru/CeO_2. Figure 2a shows the TPD spectrum for the Ru_3/CeO_2-673ev after adsorption A. D_2 and HD began to be desorbed around 330 and 450 K, respectively. This difference implied that the adsorption of hydrogen (H, D) on Ru was weak for Ru_3/CeO_2-673ev because adsorbed H in the first adsorption step in H_2 should be easily replaced by D in the second adsorption step in D_2. The origin of H atoms of desorbed HD and lesser amounts of H_2 can be

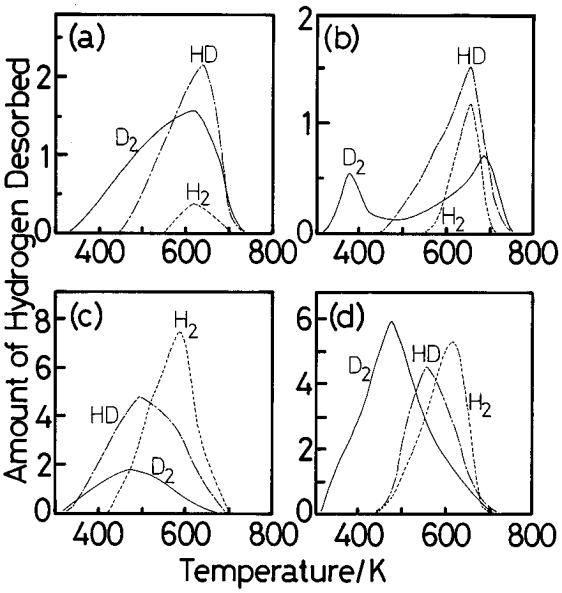

Figure 2. TPD spectra for hydrogen on Ru_3/CeO_2-673ev (a), conventional Ru/CeO_2 (b), Ru_3-Ni/CeO_2-673ev (c, d). Sample was in H_2 (76 kPa) at 293 K, evacuated at 293 K and then in D_2 (76 kPa) at 293 K (adsorption A) for parts a−c. Sample was in D_2 (76 kPa) at 293 K (adsorption B) for part d. (—) D_2; (−•−) HD; (- - -) H_2. The heating rate was 4 K min^{-1}.

ascribed to inversely spiltover H from cerium oxide surface to Ru clusters because the H(a) on cerium oxide (as hydroxyl, etc.) was desorbed only as H_2O in the absence of Ru clusters.

The order of beginning temperature of desorption (D_2 < HD < H_2) was the same for conventional Ru/CeO_2 (Figure 2b) after adsorption A. Compared to Figure 2a, the adsorption of D should be weaker on Ru particles of conventional Ru/CeO_2 to make the first maximum of D_2 desorption as low as around 390 K. The higher temperature peak of D_2 (around 690 K) may originate from inversely spiltover D by the recombination on Ru. Again after adsorption A, TPD was measured for Ru_3-Ni/CeO_2-673ev. D_2 and HD began to be desorbed at the same temperature (around 330 K) (Figure 2c). The temperature where H_2 began to be desorbed (around 430 K) was similar to those for HD in Figure 2a,b (around 450 K).

TPD was observed also for Ru_3-Ni/CeO_2-673ev after adsorption B. Around 310−450 K, only D_2 was desorbed (Figure 2d). HD and H_2 began to be desorbed around 450 K similar to HD in Figure 2a,b or H_2 in Figure 2c. The inverse hydrogen spillover (from support to Ru) should occur above 450 K also for Figure 2c,d compared to the HD desorption in Figure 2a,b. The ratio of total desorbed hydrogen amount in Figure 2 (1.2:0.70:4.0:3.8) corresponded to the uptake ratio in Table 2 (Ru_3/CeO_2-673ev:conventional Ru/CeO_2:Ru_3-Ni/CeO_2-673ev = 1.2:0.5:4.1) except for the relatively higher value for Figure 2b probably because the amount of spiltover hydrogen onto support was also included for TPD observation.

Ru Cluster Structures. *1. EXAFS. a. Incipient Cluster.* When **1** was reacted with CeO_2 in THF, the yellow solution turned transparent in 3 min, suggesting fast reaction between **1** and CeO_2. In fact, the EXAFS drastically changed on supporting on CeO_2 from EXAFS for **1**. The data for incipient Ru_3/CeO_2 were well fitted with three waves (Ru−C, Ru(−C−)O, Ru−O) with $R_f = 1.2\%$ (Table 3a). Alternative fitting with four waves (three waves and Ru−Ru) did not improve the fitting ($R_f = 2.0\%$), indicating the cleavage of Ru−Ru bonds of **1** upon the reaction with CeO_2.

b. Ru_3/CeO_2. Incipient Ru_3/CeO_2 was heated at 673 or 813 K in vacuum. The FT of the Ru K-edge EXAFS is shown in

TABLE 3: Results of Curve-Fitting Analysis of Ru K-Edge EXAFS Spectra for Ru_3/CeO_2-673ev, Ru_3/CeO_2-813ev, and Ru_3-Ni/CeO_2-673ev before/after Hydrogen Treatment at 588 K

			Ru−C		Ru−Ru		Ru(−C−)−O		Ru−O		Ru···Ru		
entry	sample	hydrogen treatment at 588 K	*N*	*r*/Å	*N*	*r*/Å	*N*	*r*/Å	*N*	*r*/Å	*N*	*r*/Å	R_f/%
a	incip Ru_3/CeO_2	before	3.1	1.95			3.0	3.00	2.0	2.10			1.2
b	Ru_3/CeO_2-673ev	before			4.4	2.62			1.5	2.04			4.7
c		after			5.4	2.62			0.6	2.14			2.4
d	Ru_3/CeO_2-813ev	before							4.7	2.02	6.2	3.37	2.1
e		after			7.0	2.61			1.1	2.08			0.6
f	Ru_3-Ni/CeO_2-673ev	after			7.1	2.62			1.2	2.12			1.7

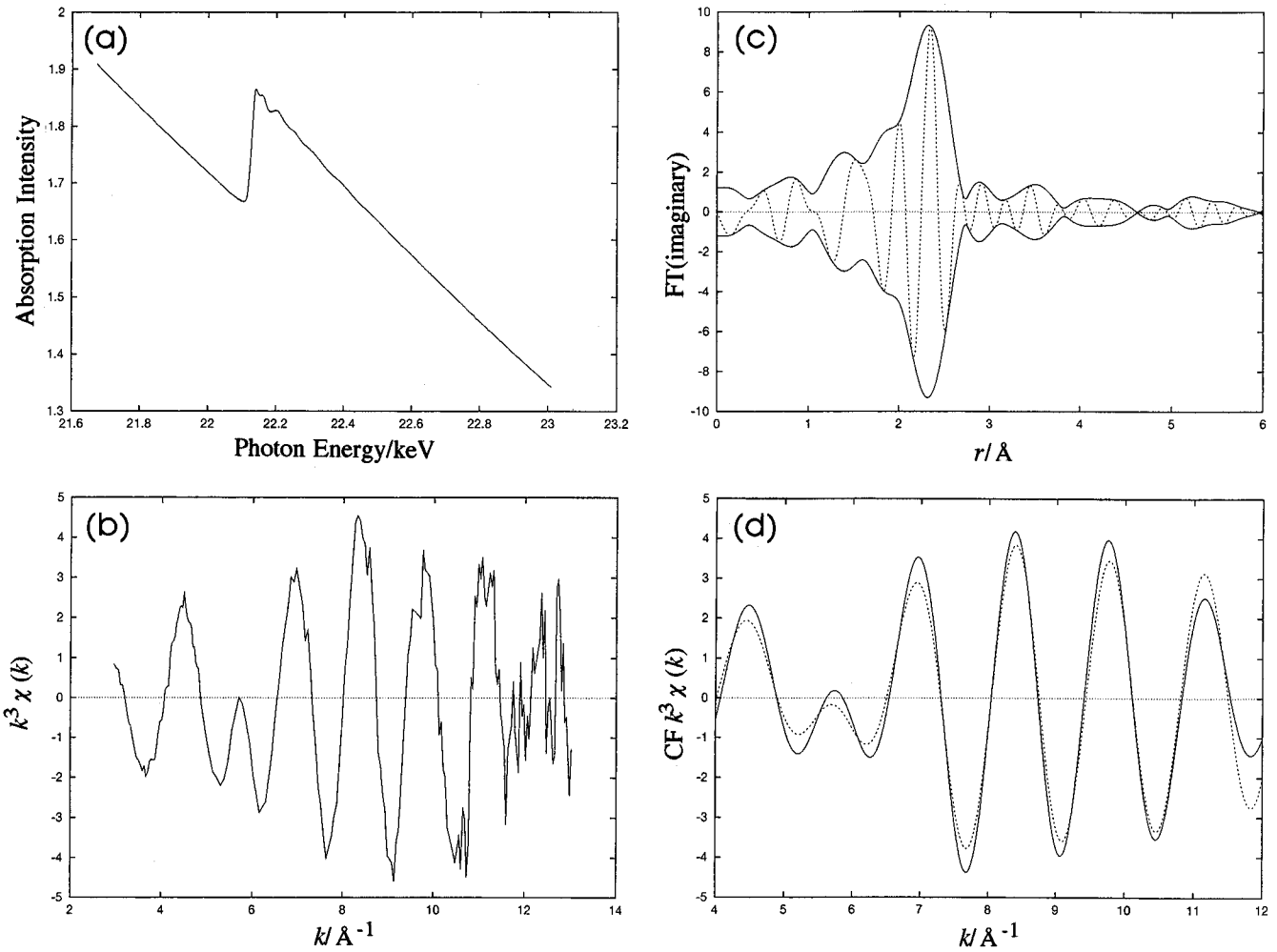

Figure 3. Ru K-edge EXAFS spectra observed at 293 K for Ru_3/CeO_2-673 ev. (a) Raw spectrum, (b) k^3-weighted EXAFS oscillation, (c) its associated Fourier transform, and (d) curve-fitting analysis. (—) Observed; (- - -) calculated.

Figure 3c for the sample heated at 673 K. The main peak around 2.4 Å (phase shift uncorrected) can be ascribed to Ru−Ru bonding. The shoulder on the lower-distance side in Figure 3c can be Ru−O(s) bonding.[2,7,8] In fact, the EXAFS was well fitted with two waves Ru−Ru and Ru−O(s) (Figure 3d). The obtained r_{Ru-Ru} (=2.62 Å in Table 3b) meant the metallic bonding compared to clusterlike distance 2.85 Å (average) for **1**.[9] The N_{Ru-Ru} (=4.4 in Table 3b) suggested the Ru cluster size of less than 10 Å.

The $k^3\chi$ oscillation in the EXAFS for Ru_3/CeO_2-813ev was slower than that in Figure 3b. The peak around 1.6 Å (phase shift uncorrected) was strongest in its FT. The curve-fitting analysis was performed with two waves Ru−O and Ru···Ru (second coordination in RuO_2 bulk). The best fit result was $r_{Ru-O} = 2.02$ Å ($N = 4.7$) and $r_{Ru\cdots Ru} = 3.37$ Å ($N = 6.2$) (Table 3d) ($r_{Ru-O} = 1.98$ Å ($N = 6$) and r_{Ru}...Ru = 3.55 Å ($N = 8$) for bulk RuO_2). The smaller value for $r_{Ru\cdots Ru}$ may be because the formed [RuO_x] particles on cerium oxide were too small to constitute regular crystals. Alternative fitting with two waves Ru−O and Ru−Ru (Ru metal) did not fit in the entire wavenumber region, excluding the possibility that the second shell around 2.5 Å was Ru−Ru bonding.

The Ru_3/CeO_2-673ev was put in H_2 at 588 K. The Ru K-edge EXAFS was fitted with Ru−Ru ($r = 2.62$ Å) and Ru−O(s) ($r = 2.14$ Å) (Table 3c). The value of $N_{Ru-Ru} = 5.4$ suggested that the cluster size was still smaller than 10 Å. $N_{Ru-O(s)}$ decreased by 0.9 and $r_{Ru-O(s)}$ increased by 0.10 Å by heating in H_2 at 588 K.

Similarly, the EXAFS was observed for Ru_3/CeO_2-813ev heated in H_2 at 588−773 K (Table 3e). These data were well fitted with two waves Ru−Ru and Ru−O(s), demonstrating the transformation of [RuO_x] into Ru metal clusters at lower than 588 K in H_2. With the increase of T_{H_2} from 588 to 773 K, the structural data did not change very much ($r_{Ru-Ru} = 2.62 \pm 0.01$ Å, $N_{Ru-Ru} = 7.0 \pm 0.6$, $r_{Ru-O(s)} = 2.08 \pm 0.01$ Å) except for the gradual increase of $N_{Ru-O(s)}$ (1.1 → 2.1).

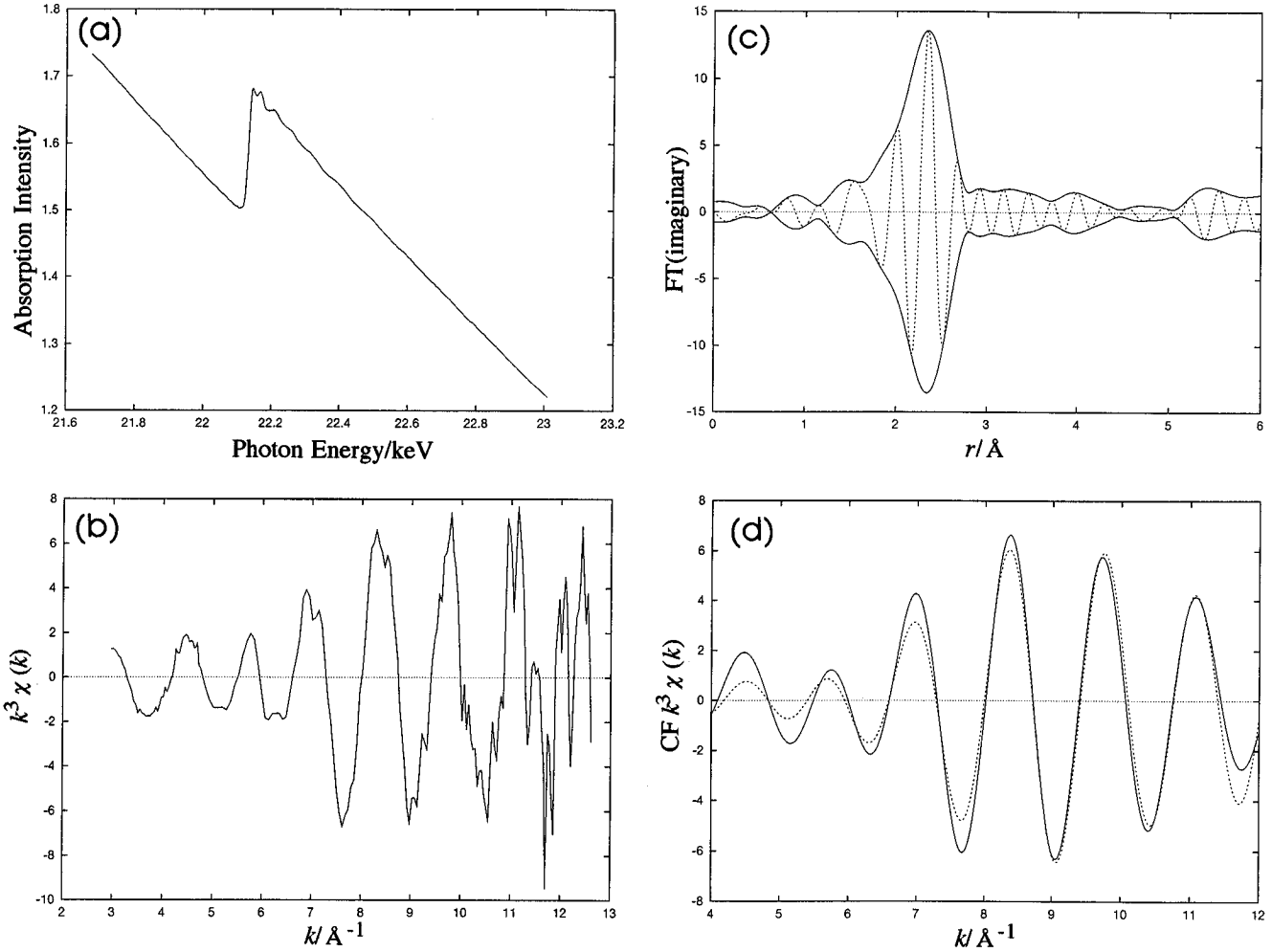

Figure 4. Ru K-edge EXAFS spectra observed at 100 K for Ru_3/CeO_2-673ev in H_2 (53 kPa). The captions for parts a−d are the same as those in Figure 3.

c. Ru_3-Ni/CeO_2. For Ru_3-Ni/CeO_2-673ev heated in H_2 at 588 K, the curve-fitting result (Table 3f) was similar to those for Ru_3/CeO_2-673ev and Ru_3/CeO_2-813ev heated in H_2 at 588 K (Table 3c,e). N_{Ru-Ru} (=7.1) was a little larger than those for corresponding samples heated in H_2 at 588 K (5.4−7.0).

d. The Interaction of Ru_3/CeO_2-673ev with H_2. In the Ru K-edge EXAFS in H_2 (53 kPa), the shoulder of Ru−O(s) bonding became weaker compared to the main peak of Ru−Ru (Figure 4c) than in the case in vacuum (Figure 3c). The curve-fitting result indicated the decrease of $N_{Ru-O(s)}$ from 1.5 to 0.6 by hydrogen adsorption. The distances r_{Ru-Ru} and $r_{Ru-O(s)}$ increased by 0.03−0.09 Å in H_2 (Table 4a,b).

2. TEM. No Ru particles were observed for Ru_3/CeO_2-673ev in H_2 at 588 K by TEM. Considering the lower limit of detection (about 12 Å), this does not contradict results with the $N_{Ru-Ru} = 5.4$ by EXAFS (Table 3c). By heating the sample in H_2 at 773 K, the average Ru particle size was 16 Å. Real average size may be smaller because the smaller (<∼12 Å) particles must not be detected. The N_{Ru-Ru} of 6.9 by EXAFS for the sample ($T_{H_2} = 773$ K) corresponds to Ru particle size of ca. 14 Å with the assumption of complete sphere shape.

In the TEM image for Ru_3-Ni/CeO_2-673ev heated in H_2 at 588 K, black particles with an average particle size of 70 Å were observed. The hydrogen uptake measurement for Ni/CeO_2 heated in H_2 at 773 K resulted in $H/Ru_{total} = 0.10$. The N_{Ru-Ru} (=7.1, Table 3f) by EXAFS corresponds to particles of 10−15 Å. Hence, it is reasonable to think that the detected particles by TEM consisted of Ni. The dispersion of Ru was calculated to be 0.55 from an average particle size of 24 Å for conventional Ru/CeO_2 by TEM (eq 1), consistent with hydrogen uptake data ($H/Ru_{total} = 0.50$) in Table 2.

Discussion

In THF at 290 K, cluster **1** was rapidly reacted with CeO_2. The EXAFS analysis ($N_{Ru-C} = 3.1$, $N_{Ru(-C-)O} = 3.0$, and $N_{Ru-O} = 2.0$ in Table 3a) and the TPD for incipient Ru_3/CeO_2 (9.3 CO desorbed per 1 Ru_3) suggested the formation of monomeric $[Ru(CO)_3(\mu\text{-}O(s)_2]$ species (Figure 5a). **1** should be reacted with Ni/CeO_2 similarly. Besides the cleavage of Ru−Ru bonds by the coordination of O(s) to $[Ru_3]$ cluster in the case of cerium oxide, the higher oxidation ability of cerium oxide surface was also evidenced as the formation of $[RuO_x]$ ($x \sim 2$) particles (Figure 5d) by heating $[Ru(CO)_3(\mu\text{-}O(s))_2]$ on cerium oxide at 813 K in vacuum (Table 3d). By heating at 673 K in vacuum, the incipient $[Ru(CO)_3(\mu\text{-}O(s))_2]$ transferred to Ru clusters of less than 10 Å (Figure 5b) on the basis of the N_{Ru-Ru} of 4.4 (Table 3b).

Reduction of Ru_3/CeO_2 and Catalysis. According to the increase of T_{H_2}, ammonia synthesis rates increased up to at T_{H_2} = 773−873 K and decreased at higher T_{H_2} than 873 K on Ru_3/CeO_2-673ev, Ru_3/CeO_2-813ev, and conventional Ru/CeO_2 (Figure 1). The corresponding curve-fitting results for EXAFS are listed in Table 3. With the increase of T_{H_2} from 588 to 873 K, N_{Ru-Ru} increased from 5.4 (Table 3c) to 9.3 for Ru_3/CeO_2-673ev, while it remained almost unchanged around 7.0 ± 0.6 for Ru_3/CeO_2-813ev (Table 3e).

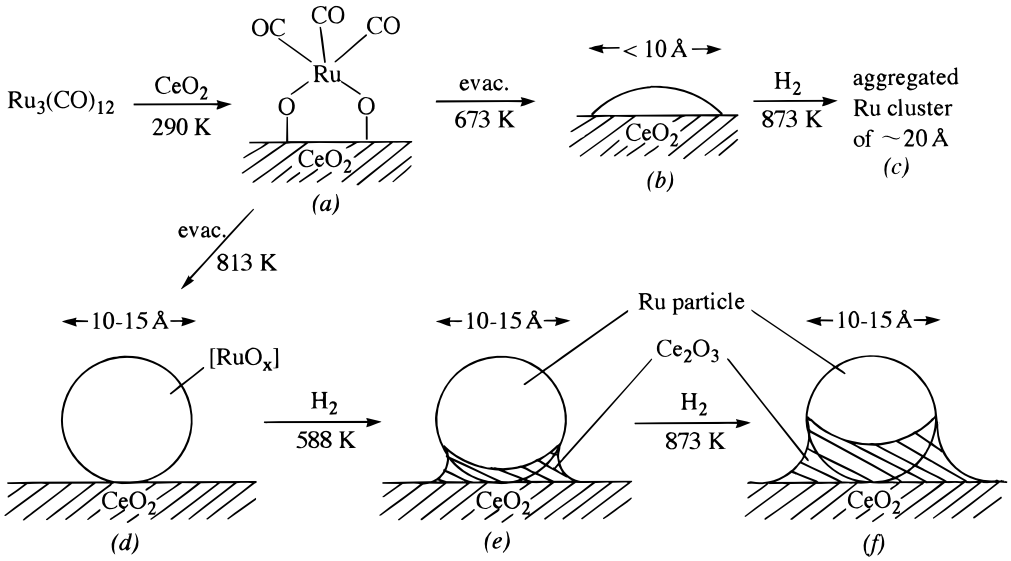

Figure 5. Active structures of supported clusters on CeO_2.

The maximum in Figure 1 can be explained by the balance of two factors. Factor A is the extent of reduction of CeO_2. The surface part of CeO_2 is reduced to transfer to Ce_2O_3 by the removal of surface or lattice oxygen. More reduced CeO_{2-x} at higher T_{H_2} was able to donate the negative charge to Ru clusters more effectively, and to facilitate the dissociative adsorption of N_2 on Ru.[3] Factor B is the number of surface Ru active sites. The number of Ru(s) decreased by the aggregation of Ru cluster as indicated by the increase of N_{Ru-Ru} according to the increase of T_{H_2} from 588 to 873 K for Ru_3/CeO_2-673ev (Figure 5b,c). In the case of Ru_3/CeO_2-813ev, $N_{Ru-O(s)}$ gradually increased from 1.1 at T_{H_2} = 588 K to 2.1 at T_{H_2} = 773 K, keeping N_{Ru-Ru} almost unchanged (Table 3e). Hence, the number of Ru(s) decreased by the growth of CeO_{2-x} at the interface by the increase of T_{H_2} (Figure 5d−f). The reduction of support was facilitated by the spiltover H from Ru clusters, and formed CeO_{2-x} at the interface may further react with interface Ru atoms to physically cover the Ru particle surface (SMSI).

On the basis of the difference of $N_{Ru-O(s)}$ (>2.1 and 0.3, respectively), the extent of Ru site blocking by CeO_{2-x} was the major reason for lower maximum rate for Ru_3/CeO_2-813ev than that for Ru_3/CeO_2-673ev (Table 1). The optimum T_{H_2} was lower by about 100 K for conventional Ru/CeO_2 than the other two. This difference may be because both Ru particle growth and the blocking of Ru site by CeO_{2-x} inhibited catalysis in conventional Ru/CeO_2.

Reduction of Ru_3−Ni/CeO_2 and Catalysis. In the catalyst preparation, the amount of hydrogen consumption was 5.04×10^{-4} mol of H_2 g_{cat}^{-1} for Ni/CeO_2 in H_2 at 773 K for 12 h: 17.4% of incipient CeO_2 was converted to Ce_2O_3 ($CeO_2 \rightarrow CeO_{1.91}$). The stoichiometry $CeO_{1.90}$ was reported by the thermogravimetry after heating CeO_2 powder in H_2 at 773 K.[10] The particles around 70 Å were detected by TEM, and H/Ni uptake measurement (0.10) also supported the data. On the other hand, the Ru cluster size of Ru_3−Ni/CeO_2-673ev in H_2 at 588 K was estimated to be 10−15 Å on the basis of N_{Ru-Ru} = 7.1 (Table 3f). As the Ru−O(s) bonds were observed by EXAFS (Table 3f), the Ni and Ru clusters should be attached on the cerium oxide surface separately. Geometrically, it is not likely that the Ru clusters bonded to the larger Ni particles also coordinate to O(s) of cerium oxide with average $N_{Ru-O(s)}$ of 1.2. The EXAFS curve-fitting analysis in Table 3f without Ru−Ni bonds should be valid.

As expected from higher reduction extent of support Ni/CeO_2, the ammonia synthesis rates were best on Ru_3−Ni/CeO_2-673ev (Figure 1). The number of surface Ru sites should have decreased by the growth of Ru particles at higher T_{H_2} (factor B), resulting in the rate decrease, while factor A was kept unchanged because the reduction temperature in catalyst preparation for Ni/CeO_2 was higher (=773 K).

Hydrogen Adsorption on Ru_3/CeO_2 and Ru_3−Ni/CeO_2. The hydrogen uptake measurements (Table 2) and TPD observations for hydrogen (Figure 2) indicated that the H/Ru_{total} exceeded 1 for Ru_3/CeO_2-673ev and Ru_3−Ni/CeO_2-673ev. Excessive amounts of hydrogen adsorption are reported for Ru/SiO_2 (H/Ru(s) = 3.3−5.6),[5] Rh/Al_2O_3 (H/Rh(s) = 0.70−1.39),[11] Rh/CeO_2 (H/Rh_{total} = 0.75−3.97),[12] or Pt/zeolite (H/Ru_{total} = 1.4−1.7).[13]

The TPD were observed for samples after adsorption A (Figure 2a−c) and adsorption B (Figure 2d). In the range of 300−450 K (region I), D_2 was exclusively desorbed in Figure 2a,b,d. In these three spectra, the incorporation of H (as HD for Figure 2a,b,d and as H_2 for Figure 2d) began at ~450 K, in good coincidence. It should be noted that only Figure 2c had HD desorption in region I and that the total desorption amount (H_2 + HD + D_2) was larger in Figure 2c,d than in Figure 2a,b by the factor of 3.2−5.7 (the *y*-axes in Figure 2 are common on the basis of per gram of catalyst). Hence, we believe that the Ru_3−Ni/CeO_2 had a different kind of adsorption site for H, compared to the Ru_3/CeO_2 or conventional Ru/CeO_2.

The H incorporation in region II (450−750 K) seems due to inverse hydrogen spillover, similar to H spillover initiated at ~413 K on Rh/TiO_2.[4] The inversely spiltover H should have reacted with D on Ru sites to form HD (Figure 2a,b). However, Ru_3−Ni/CeO_2 had again different desorption character. Namely, a significant amount of H_2 was also desorbed in region II of Figure 2c besides HD. The total desorption curve of HD + D_2 in Figure 2c was similar to that of D_2 in Figure 2d.

Taking these facts into account, we propose an interface adsorption site for H in the case of Ru_3−Ni/CeO_2. The H on this new site was not replaced by D even in D_2 (second adsorption step before TPD for Figure 2c), different from replaceable H on ordinary Ru sites where only D_2 was desorbed as in region I of Figure 2a or Figure 2b. This new site for H on Ru_3−Ni/CeO_2 should be different from ordinary Ru sites (D_2 in region I) or cerium oxide surface sites (H as HD or H_2 in region II). The H of HD in region I in Figure 2c can be

TABLE 4: Results of Curve-Fitting Analysis of Ru K-Edge EXAFS Spectra for Ru_3/CeO_2-673ev in Vacuum or in H_2 (53 kPa)

			Ru−Ru			Ru−O			
entry	T_{H_2}/K	ambient gas	N	r/Å	$\Delta(\sigma^2)/10^{-3}$ Å^2	N	r/Å	$\Delta(\sigma^2)/10^{-3}$ Å^2	R_f/%
a		vacuum[a]	4.4 (±0.7)	2.62 (±0.02)	2.8	1.5 (±0.4)	2.04 (±0.03)	5.6	4.7 (±2.4)
b		H_2[b]	4.5 (±0.6)	2.65 (±0.02)	0.45	0.6 (±0.3)	2.13 (±0.02)	−0.6	3.8 (±1.9)
c	588	vacuum[a]	5.4	2.62	2.9	0.6	2.14	−5.6	2.4
d		H_2[a]	5.5	2.65	0.8	0.7	2.14	−4.7	2.3

[a] Observed at 290 K. [b] Observed at 100 K.

understood to be derived from this new site, in equilibrium with D(a) on ordinary Ru sites at >∼330 K on the basis of the coincidence of the beginning temperatures of HD and D_2 desorption in Figure 2c (∼330 K). The reason why H_2 was not formed in region I of Figure 2c besides HD and D_2 is unclear. The very fast recombination of H from the proposed new site with D(a) on Ru sites near the interface may be the reason.

Figures 4 and 5 show the structure change for Ru clusters of Ru_3/CeO_2-673ev by interaction with H_2. The bonding distances r_{Ru-Ru} (2.62 Å) and $r_{Ru-O(s)}$ (2.04 Å) in vacuum were enlarged by 0.03 and 0.09 Å, respectively, in H_2 (Table 4a,b). The relaxation induced by H adsorption was also observed for Ru_3/CeO_2-673ev heated in H_2 at 588 K. $r_{Ru-O(s)}$ was already enlarged to 2.14 Å by heating in H_2 at 588 K (Table 4c), and it did not show further change by hydrogen adsorption (Table 4d). The r_{Ru-Ru} changed from 2.62 to 2.65 Å by H adsorption, same as the change by the H adsorption on Ru_3/CeO_2-673ev (Table 4a,b). The relaxation of metal cluster by hydrogen adsorption was reported for supported Ru catalysts (Δr_{Ru-Ru} = 0.03−0.08 Å and $\Delta r_{Ru-O(s)}$ = 0.03−0.04 Å)[2] and supported Pt catalysts (Δr_{Pt-Pt} = 0.12−0.19 Å).[14]

Adsorption Sites of Excessive Hydrogen. *1. Weakly Bound Hydrogen.* Weakly bound H was proposed on metal catalysts by using NMR: part of a peak around 0 ppm on Rh/TiO_2[4] and peak β around −30 ppm on Ru/SiO_2.[5] In comparison between two Ru/SiO_2 samples ($Ru(s)/Ru_{total}$ = 0.29 and 0.19), "weakly bound H" was implied to have an interaction with lower coordination Ru sites because the β peak population increased as the Ru particle size decreased. The dispersions of Ru in this study were nearly 100% except for conventional Ru/CeO_2. "Weakly bound H" on lower coordination Ru atoms or hydrogen overlayer was possible as a new site for H discussed above because the largest average Ru particles (24 Å by TEM) for conventional Ru/CeO_2 are still smaller than those for Ru/SiO_2 in NMR study.

2. Hydrogen Absorption in Ru. Another possibility is the subsurface hydrogen incorporation.[15,16] On the basis of the N_{Ru-Ru} = 4.4 by EXAFS for Ru_3/CeO_2-673ev (Table 3b), a monolayer-like flat Ru cluster (packed cluster of 4 atoms × 4 atoms has an average N_{Ru-Ru} of 4.3) or octahedral 6-Ru (*or* a little larger) cluster (N_{Ru-Ru} of 4) is postulated on supports. In these plausible small clusters, almost no space for hydrogen incorporation remains. The larger $N_{Ru-O(s)}$ (=1.5) for Ru_3/CeO_2-673ev (Table 3b) suggests a flat structure of Ru clusters (Figure 5b) rather than a spherical structure. $N_{Ru-O(s)}$ was 1.2 for Ru_3-Ni/CeO_2-673ev (Table 3f), also suggesting flat Ru morphology. H incorporated in Ru bulk sounds very unlikely as a new site for H.

3. Interface Site for Hydrogen. The H uptake on Ru_3-Ni/CeO_2-673ev was 4.3 H per total Ru atoms (Table 2), and subsequent TPD had concomitant HD and H_2 desorption below 450 K (Figure 2). These facts suggest the new site for H is closely related to the reduction of cerium oxide support. Adsorbed hydrogen was monitored by FTIR; however, we could not discriminate between "weakly bound H" and "interface site H" (see the Appendix).

Relevance to Catalysis. The reaction mechanism of ammonia synthesis on Ru catalysts was investigated.[1,3,17] No N_2 adsorption was reported on Ru/MgO (183 K) or $Ru-Cs^+/MgO$ (293 K) in $N_2 + H_2$. The adsorbed amount of N_2 per Ru(s) decreased drastically when the adsorbed H increased for $Ru-Cs^+/MgO$ at 293 K. These results demonstrated preferable adsorption of H on surface Ru sites rather than N_2.[1] In fact, P_{H_2} pressure dependence of ammonia synthesis rate was −0.5 to +0.5 for Ru catalysts compared to ∼1.5 for Fe catalysts,[3,17] demonstrating that adsorbed H retarded catalysis by the strong blocking of Ru active sites not to afford enough ensemble sites for N_2 dissociative adsorption for Ru catalysts.

In the TPD for Ru_3-Ni/CeO_2-673ev (Figure 2c), the ratio of HD and D_2 desorption was about 2:1 (D/H ∼ 2) in region I, in fast equilibrium of hydrogen between the "new site" (interface H site or weakly bound H site) and normal Ru surface sites. In region II of Figure 2c, the peak ratio of HD/H_2 was about 1:1. The stronger intensity of H_2 peak than HD peak in Figure 2c compared to in Figure 2a or Figure 2b suggests that the H_2 was not only native to H(a) on cerium oxide but was also native to the new site H. The new site H was still exchangeable with D(a) on the Ru cluster surface in region II. As the ammonia synthesis temperature (588 K) was within region II, about half or an equivalent amount of new site hydrogen may be in equilibrium with hydrogen on surface Ru active sites on the basis of the D/H ratios. The contribution of the new H site can be one important factor for catalysis as a "reservoir" of reactant.

Conclusions

The Ru cluster supported on reduced Ni/CeO_2 was a good catalyst for ammonia synthesis. The Ru cluster size was less than 10 Å and within 10−15 Å for Ru_3/CeO_2 and Ru_3-Ni/CeO_2, respectively. The Ru−O(s) bondings were observed at 2.02−2.14 Å for these catalysts. The flat Ru clusters were suggested as active sites. The amounts of hydrogen uptake exceeded unity for Ru_3/CeO_2 and Ru_3-Ni/CeO_2, and H on the new site was proposed in relation to an excess amount of H uptake and subsequent TPD for H(a). The interface between Ru clusters and the reduced CeO_{2-x} surface is one possible new site.

Acknowledgment. This research was supported by a Grant-in-Aid for Scientific Research (No. 05225206) from the Ministry of Education, Science, and Culture.

Appendix

FTIR. FTIR spectra of Ru_3-Ni/CeO_2 and Ni/CeO_2 were recorded on a FTIR spectrometer (JASCO, Valor III, resolution 1 cm^{-1}).[3] CeO_2 with higher surface area (165 m^2 g^{-1}, Anan Kasei Co.) was used. Five peaks were observed at 3687m, 2206w, 2087w, 1947vw, and 1895w cm^{-1} for Ru_3-Ni/CeO_2-673ev in H_2 at 203 K for 30 min (Figure A1 in the supporting information). Compared to the spectrum in H_2 for 5 min, three peaks at 3687, 1947, and 1895 cm^{-1} grew stronger as the time passed in H_2. Three peaks around 3687, 2206, and 2087 cm^{-1} were also seen for Ni/CeO_2. Ru_3-Ni/CeO_2-673ev was evacu-

ated and in D_2 for 30 min. A new peak appeared at 2675 cm^{-1}, and two peaks at 1947 and 1895 cm^{-1} disappeared.

The peak at 3687 cm^{-1} can be assigned to hydroxyl on the cerium oxide surface because it shifted to 2675 cm^{-1} in D_2. The two peaks at 2206 and 2087 cm^{-1} may arise from electronic transitions for Ce^{3+}.[18] The remaining two peaks at 1947 and 1895 cm^{-1} may be assigned to H on (or near) Ru clusters based on Table 3 of ref 3 or Table 1(a) of ref 1. The proposed new site (see Discussion) for H may be at the interface between Ru clusters and cerium oxide surface as detected around 3687 cm^{-1} in FT-IR, probably overlapping ordinary surface hydroxyl groups.

X-ray Photoelectron Spectroscopy (XPS). XPS was measured by ESCALAB 202I (VG). The catalyst sample (powder) was sealed off from the glass vacuum system in a glass ampule and transferred inside the ESCALAB without contact with air. The peak of C 1s was taken as the standard of binding energy (=284.5 eV). In Table A1 (see the supporting information) compared to the Ru $3p_{3/2}$ peak for neutral Ru powder at 462.0 eV, the Ru $3p_{3/2}$ peak was at lower binding energy by 0.7 eV for Ru_3/CeO_2-673ev in H_2 at 588 K and by 1.3 eV for Ru_3−Ni/CeO_2-673ev in H_2 at 588 K. It should be noted that conventional Ru/CeO_2 had a main neutral peak at 462.0 eV and a weaker shoulder peak at 461.1 eV.

Supporting Information Available: Table A1 lists XPS binding energies for Ru catalysts, and Figure A1 shows the FTIR spectra of Ru_3-Ni/CeO_2-673ev and Ni/CeO_2 in H_2 (2 pages). Ordering information is given on any current masthead page.

References and Notes

(1) Izumi, Y.; Hoshikawa, M.; Aika, K. *Bull. Chem. Soc. Jpn.* **1994**, *67*, 3191.
(2) Izumi, Y.; Aika, K. *J. Phys. Chem.* **1995**, *99*, 10336.
(3) Izumi, Y.; Aika, K. *J. Phys. Chem.* **1995**, *99*, 10346.
(4) Sanz, J.; Rojo, J. M. *J. Phys. Chem.* **1985**, *87*, 4974.
(5) Bhatia, S.; Engelke, F.; Pruski, M.; Gerstein, B. C.; King, T. S. *J. Catal.* **1994**, *147*, 455.
(6) Murata, S.; Aika, K. *J. Catal.* **1992**, *136*, 118.
(7) Izumi, Y.; Chihara, T.; Yamazaki, H.; Iwasawa, Y. *J. Phys. Chem.* **1994**, *98*, 594.
(8) Izumi, Y.; Iwasawa, Y. *CHEMTECH* **1994**, *24* (July), 20.
(9) Churchill, M. R.; Hollander, F. J.; Hutchinson, J. P. *Inorg. Chem.* **1977**, *16*, 2655.
(10) Fierro, J. L. G.; Soria, J.; Sanz, J.; Rajo, J. M. *J. Solid State Chem.* **1987**, *66*, 154.
(11) Wanke, S. E.; Dougharty, N. A. *J. Catal.* **1972**, *24*, 367.
(12) Bernal, S.; Botana, F. J.; Calvino, J. J.; Cauqui, M. A.; Cifredo, G. A.; Jobacho, A.; Pintado, J. M.; Izquierdo, J. M. *J. Phys. Chem.* **1993**, *97*, 4118.
(13) Vaarkamp, M.; Modica, F. S.; Miller, J. T.; Koningsberger, D. C. *J. Catal.* **1993**, *144*, 611.
(14) Renouprez, A.; Touilloux, P.; Moraweck, B. *Growth and Properties of Metal Clusters*; Bourdon, J., Ed.; Elsevier: Amsterdam, The Netherlands, 1980; p 421.
(15) Yates, Jr., J. T.; Peden, C. H. F.; Houston, J. E.; Goodman, D. W. *Surf. Sci.* **1985**, *160*, 37.
(16) Held, G.; Pfnur, H.; Menzel, D. *Surf. Sci.* **1992**, *271*, 21.
(17) Aika, K.; Kumasaka, M.; Oma, T.; Kato, O.; Matsuda, H.; Watanabe, N.; Yamazaki, K.; Ozaki, A.; Onishi, T. *Appl. Catal.* **1986**, *28*, 57.
(18) Binet, C.; Badri, A.; Lavalley, J. *J. Phys. Chem.* **1994**, *98*, 6392.
(19) Nefedov, V. I. *X-ray Photoelectron Spectroscopy of Solid Surface*; VSP BV: Utrecht, 1988.

JP952602O